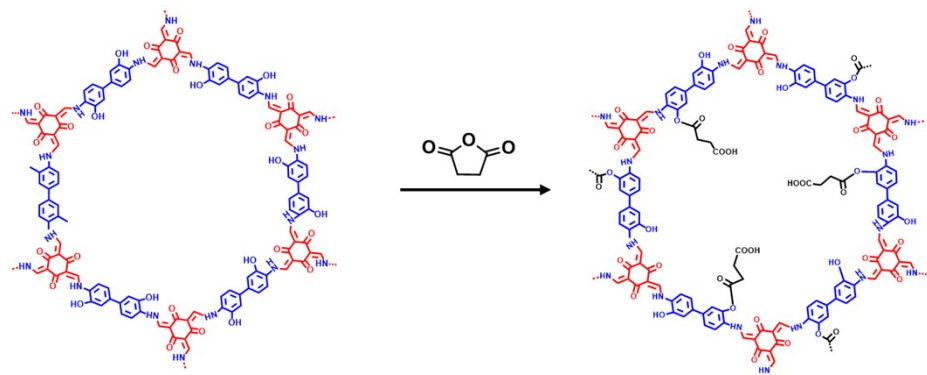


## Electronic Supplementary Information

### **Ultrathin heterostructured covalent organic framework membranes with interfacial molecular sieving capacity for fast water-selective permeation**

*Hao Yang, Hong Wu\*, Yumeng Zhao, Meidi Wang, Yimeng Song, Xuanxuan Cheng, Hongjian Wang, Xingzhong Cao, Fusheng Pan\* & Zhongyi Jiang\**

## Supplementary Figures



**Fig. S1.** The post-modification reaction for synthesizing COF CTpDHBD.

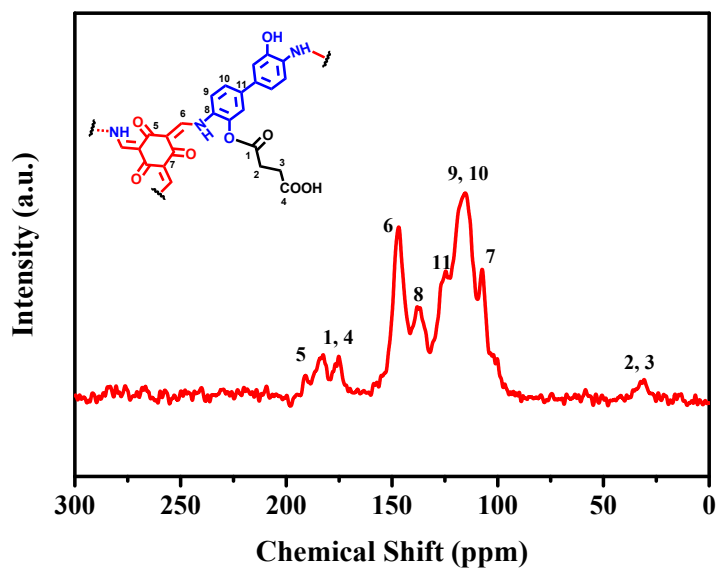


**Fig. S2.**  $^{13}\text{C}$  CP/MAS NMR spectrum of CTpDHBD.

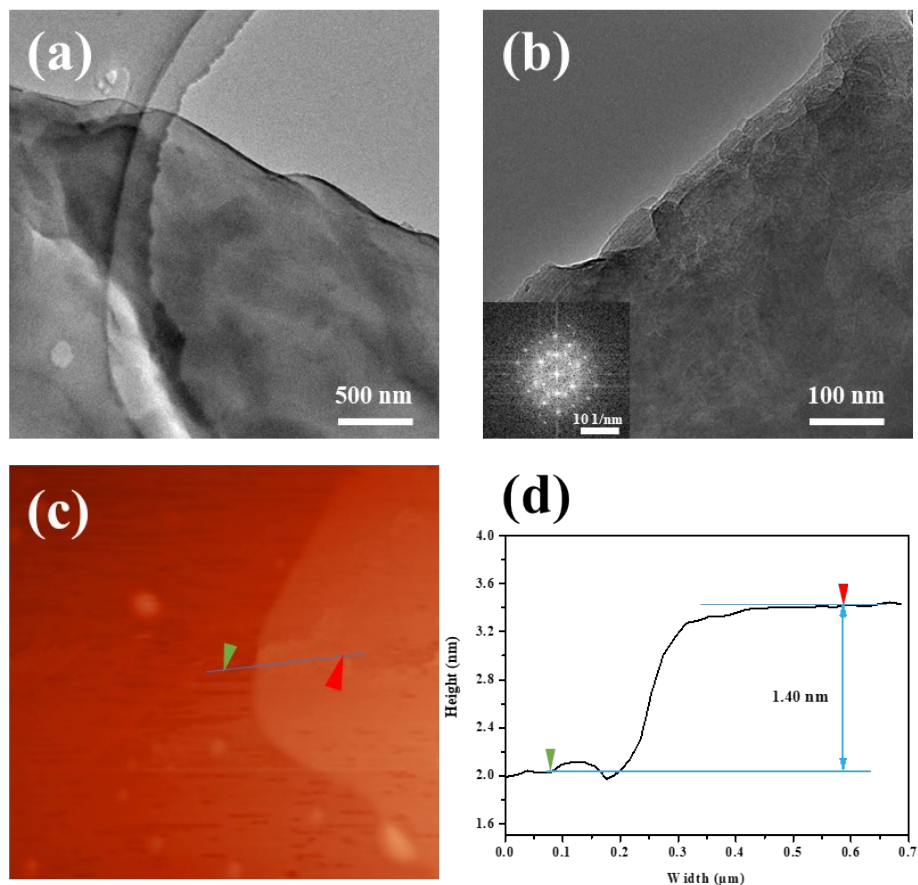


**Fig. S3.** (a) TEM image of CTpDHBD. (b) High-resolution TEM image of CTpDHBD with an inset of selected area electron diffraction (SAED) pattern. (c) AFM image and (d) height profile of CTpDHBD.

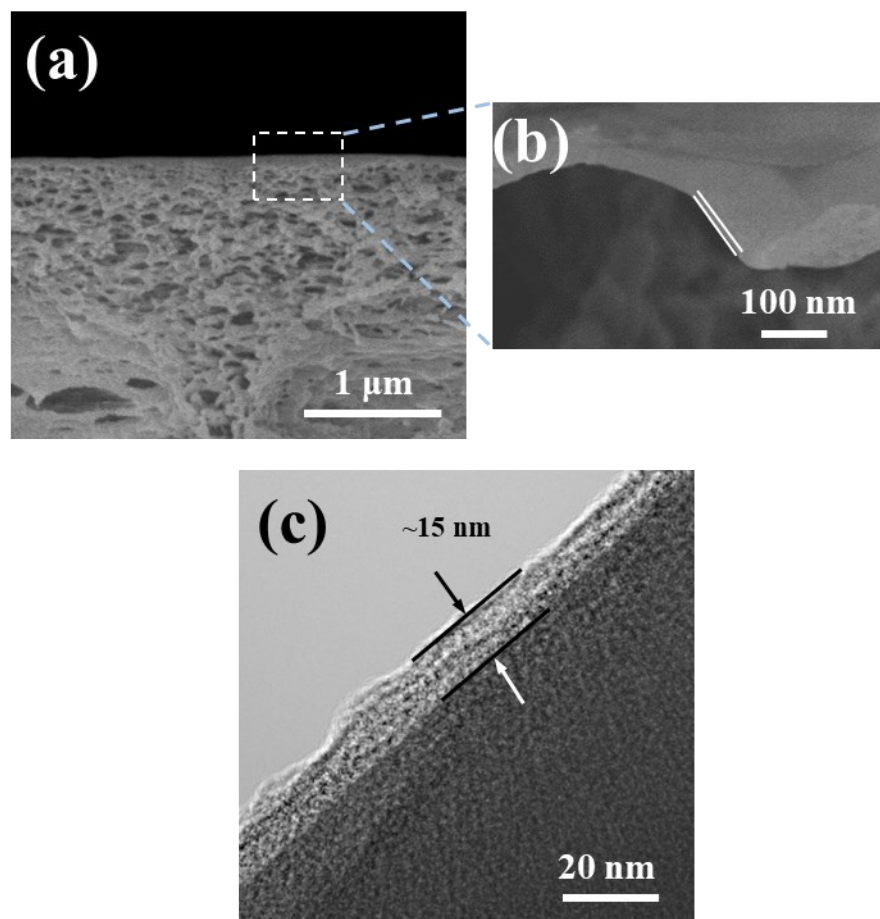
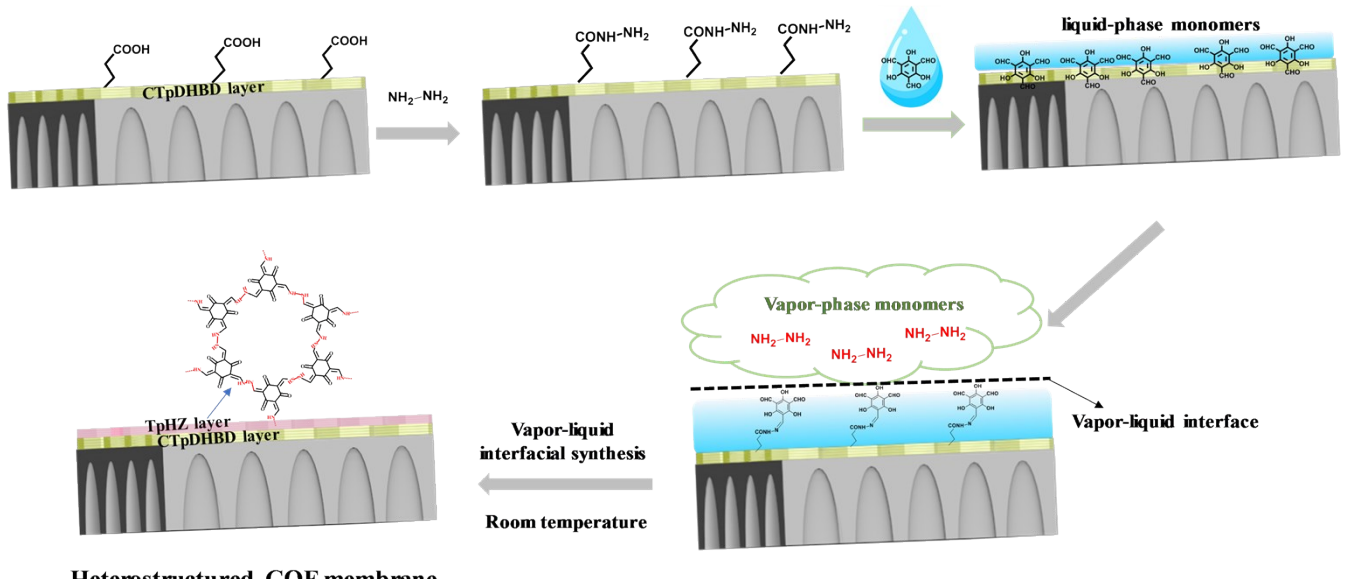


**Fig. S4.** (a) Cross-sectional FESEM image of the CTpDHBD membrane (COF content=  $0.005 \text{ g m}^{-2}$ ) with a partially enlarged image of the (b) COF layer. (c) Cross-sectional TEM image of the CTpDHBD membrane (COF content=  $0.005 \text{ g m}^{-2}$ ).



Heterostructured COF membrane

**Fig. S5.** Schematic of the vapor-liquid interfacial synthesis of TpHZ layer.

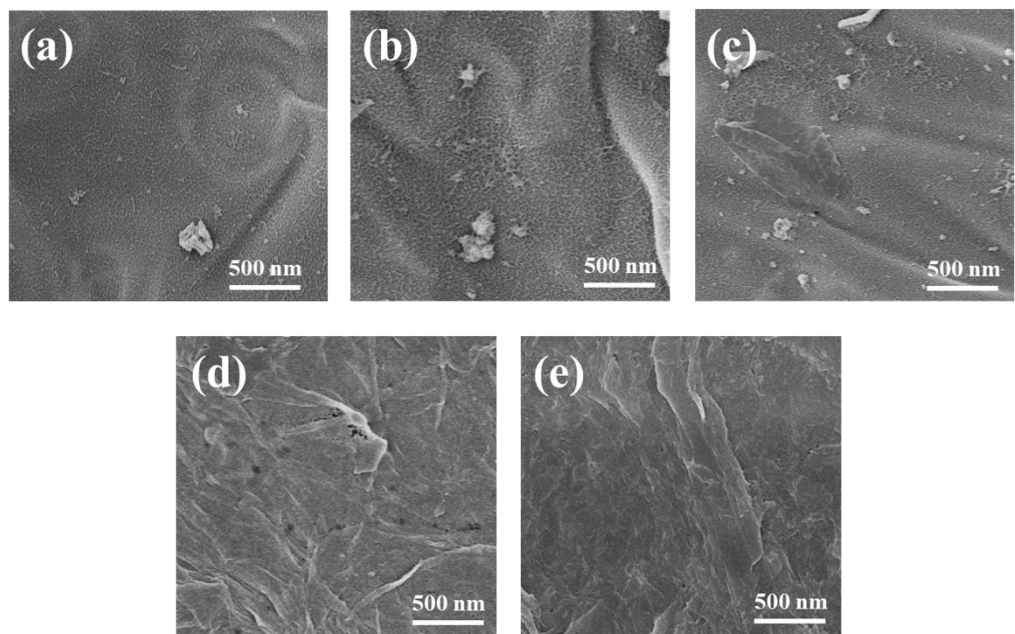


**Fig. S6.** Surface SEM images of TpHZ@CTpDHBD membranes with the vapor-liquid interfacial synthesis reaction time of (a) 24 h, (b) 36 h, (c) 48 h and (d) 60h and (e) 72 h.

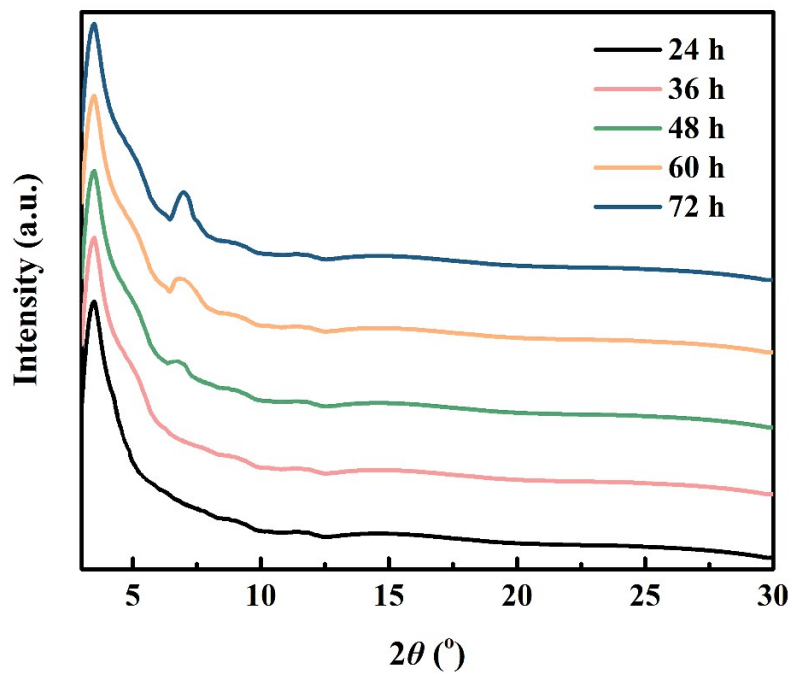


**Fig. S7.** XRD patterns of the heterostructured COF membranes with different vapor-liquid interfacial synthesis reaction time.

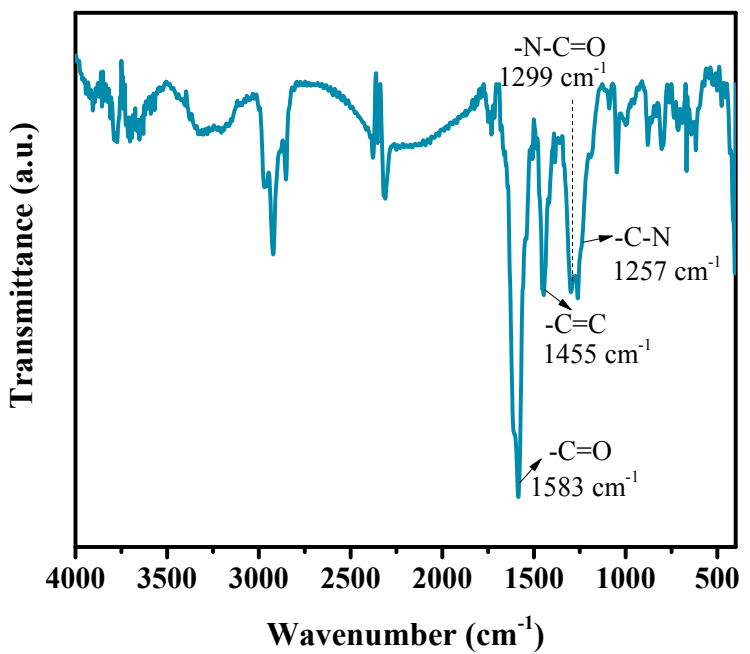


**Fig. S8.** FTIR spectrum of the heterostructured COF membrane.

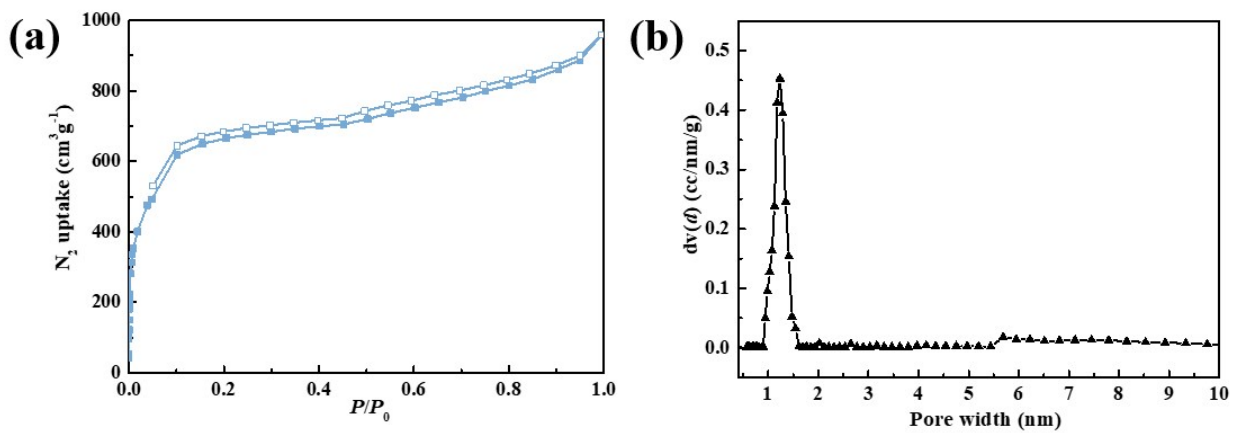


**Fig. S9.** (a)  $N_2$  adsorption-desorption isotherms and (b) PSD curve of CTpDHBD.

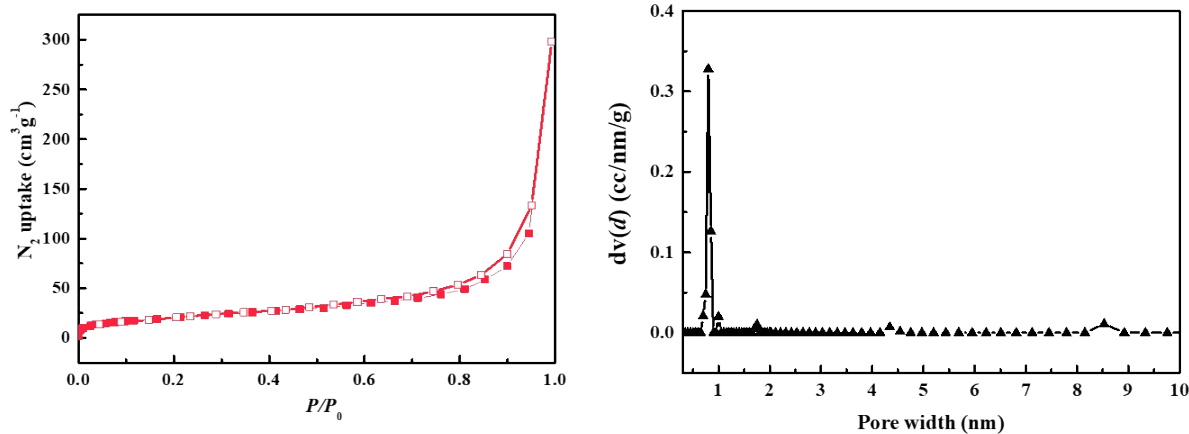


**Fig. S10.** (a)  $N_2$  adsorption-desorption isotherms and (b) PSD curve of TpHZ.

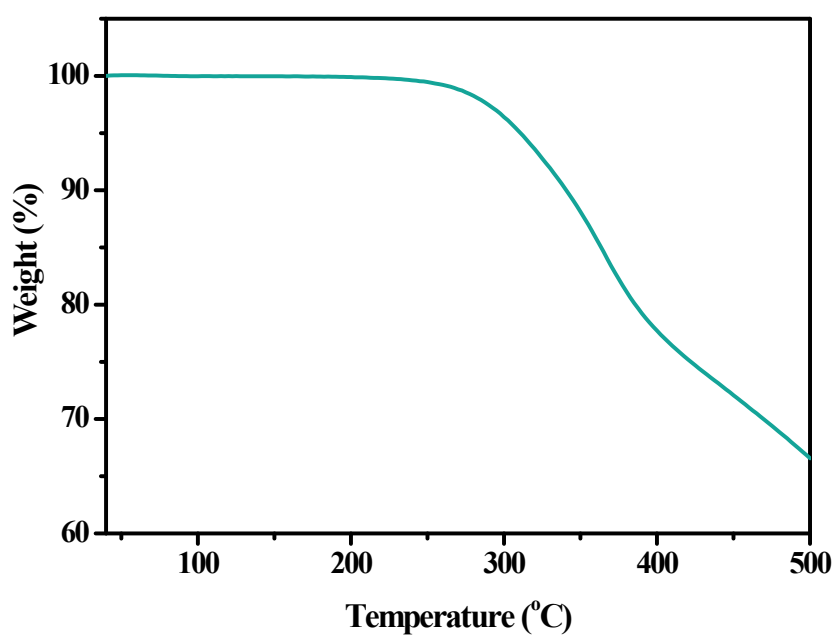


**Fig. S11.** TGA curve of the TpHZ@CTpDHBD membrane.

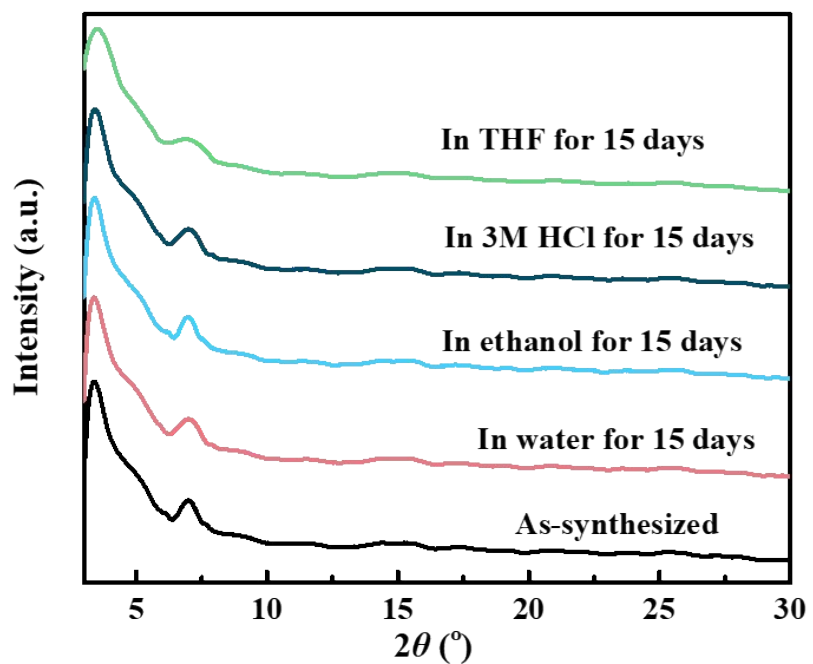


**Fig. S12.** XRD patterns of the TpHZ@CTpDHBD membranes treated in different solvents for 15 days.

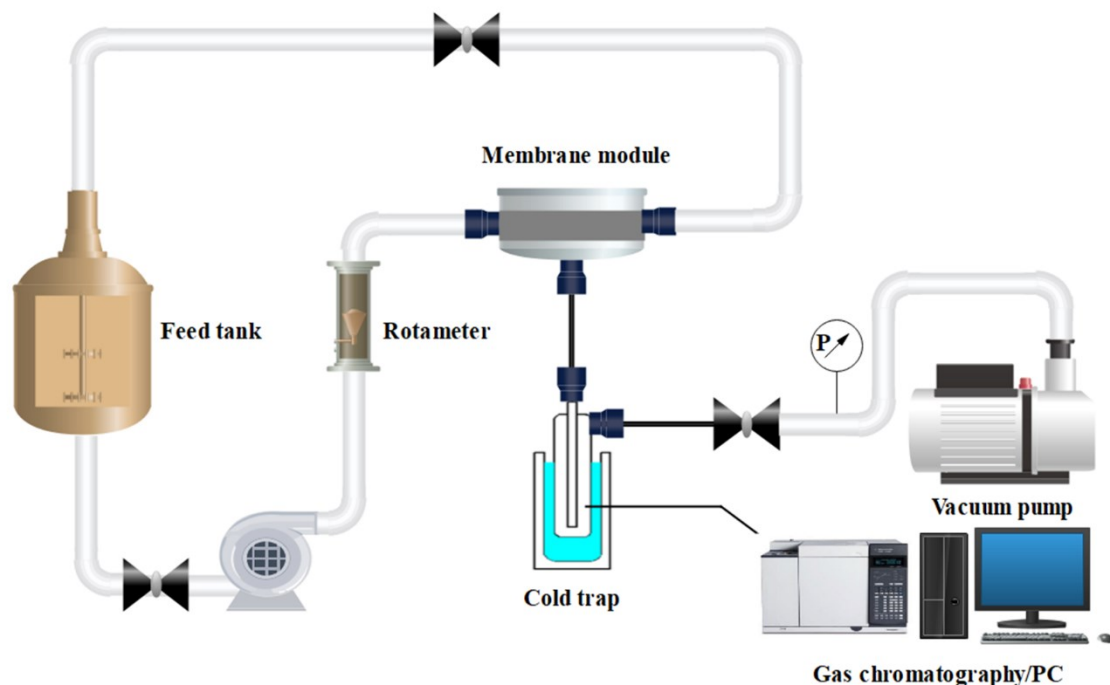


**Fig. S13.** Schematic diagram of the pervaporation experiments for water/alcohol separation.<sup>1</sup>

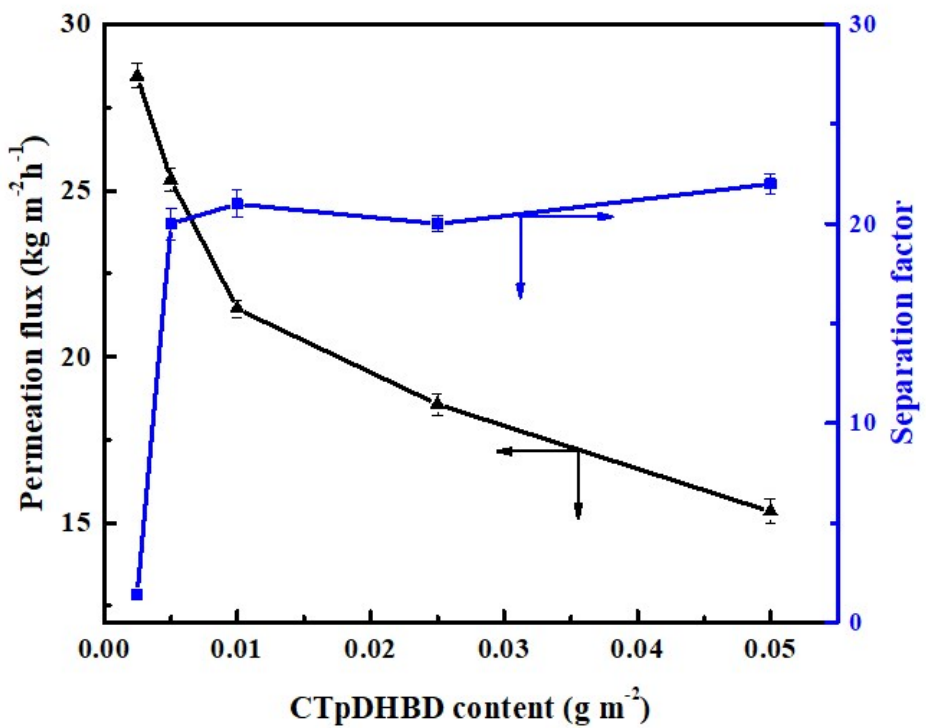


**Fig. S14.** Water/n-butanol separation performance of the single-layer CTpDHBD membranes with different COF content.

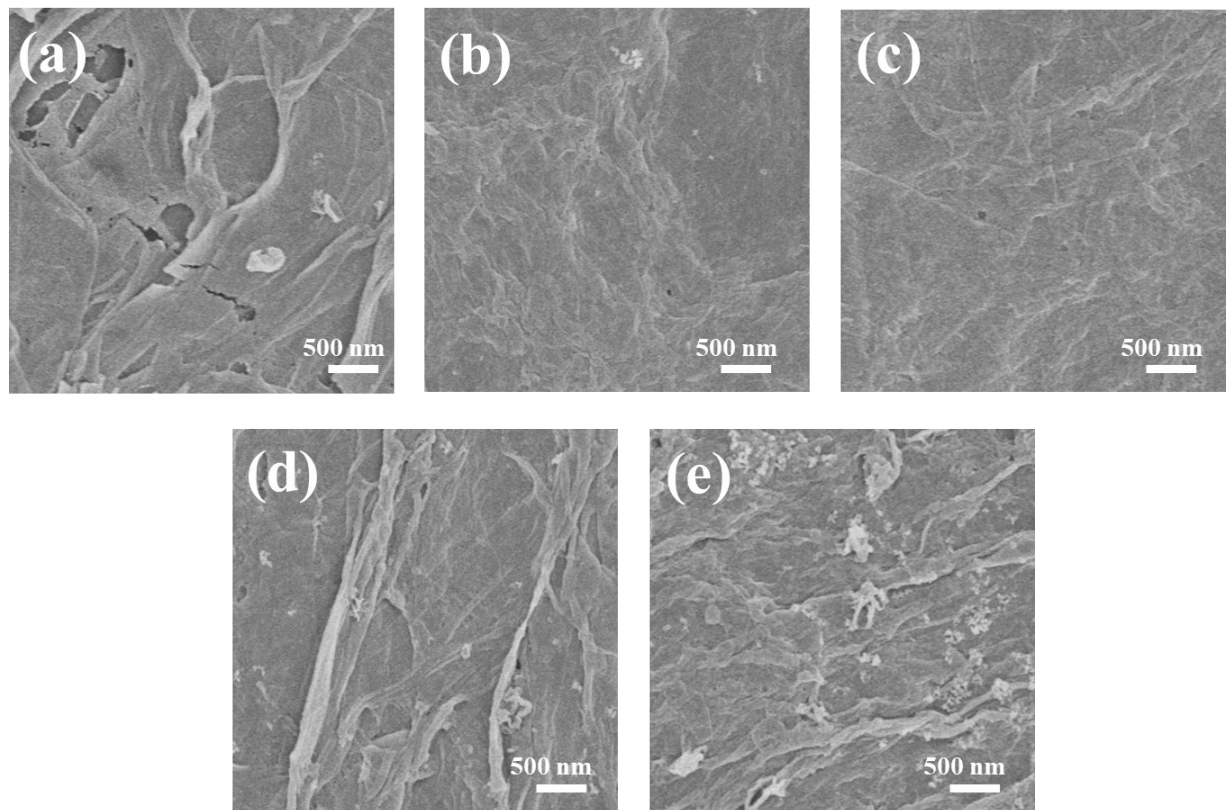


**Fig. S15.** Surface FESEM images of the heterostructured membranes with different reactive Tp concentration: (a)  $0.005 \text{ mg mL}^{-1}$ , (b)  $0.0075 \text{ mg mL}^{-1}$ , (c)  $0.01 \text{ mg mL}^{-1}$ , (d)  $0.025 \text{ mg mL}^{-1}$  and (e)  $0.05 \text{ mg mL}^{-1}$ .

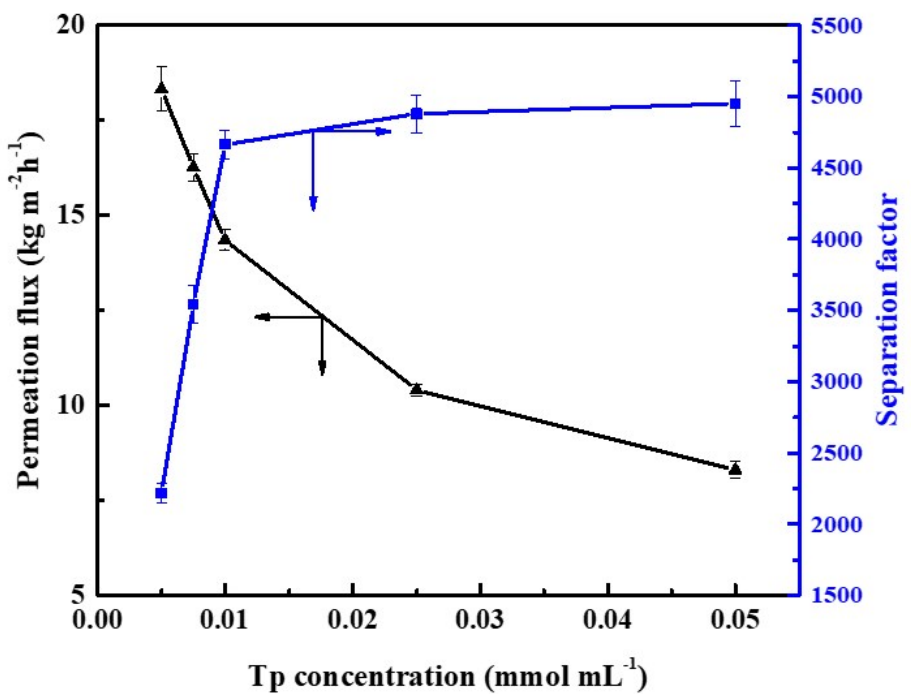


**Fig. S16.** Water/n-butanol separation performance of the heterostructured COF membranes with different reactive Tp concentration.

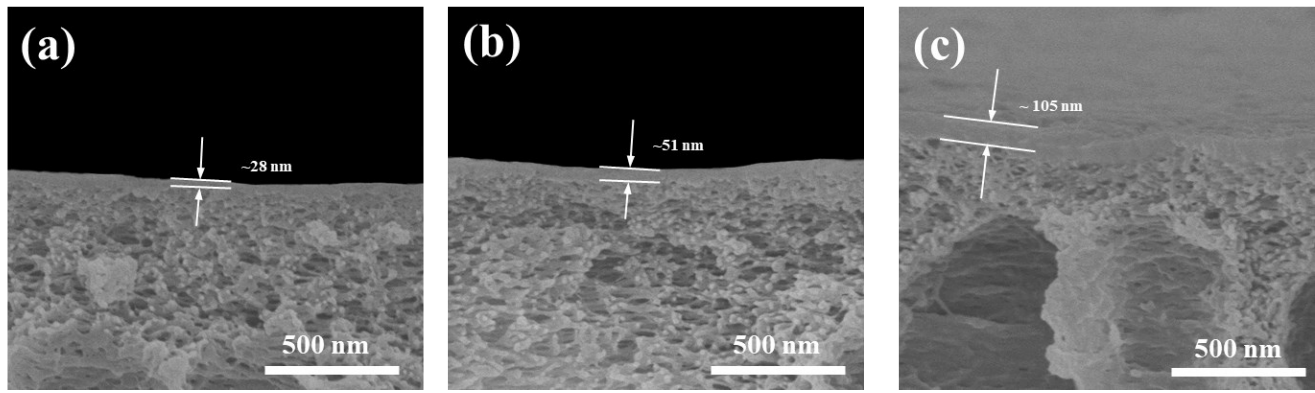


**Fig. S17.** Cross-sectional FESEM images of the heterostructured membranes with different reactive Tp concentration: (a) (a)  $0.01 \text{ mg mL}^{-1}$ , (b)  $0.025 \text{ mg mL}^{-1}$  and (c)  $0.05 \text{ mg mL}^{-1}$ .

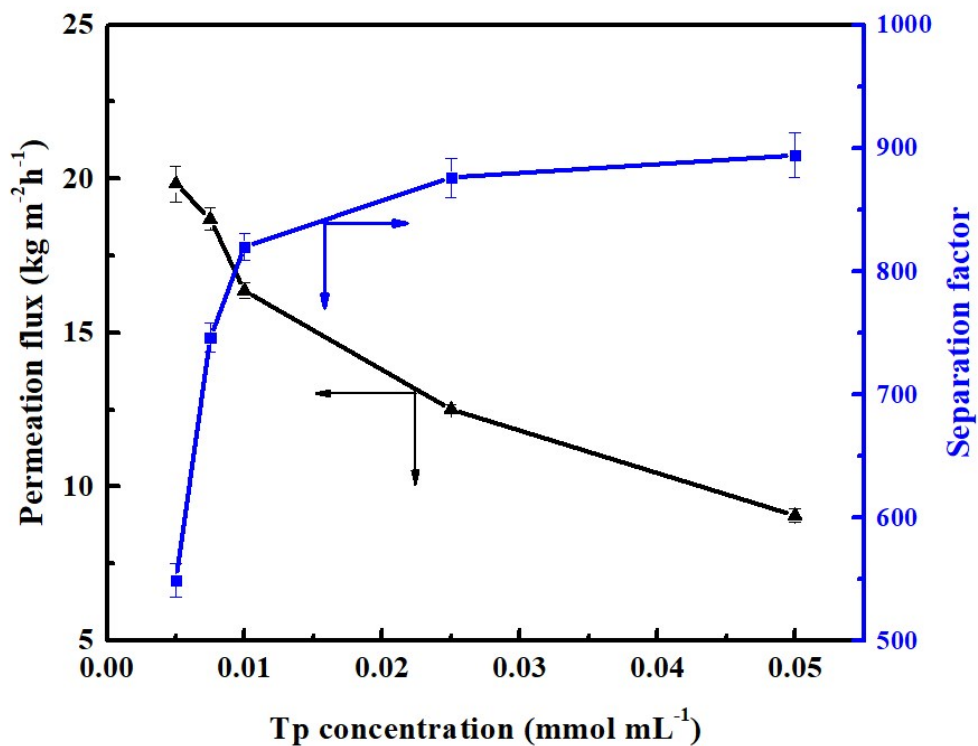


**Fig. S18.** Water/n-butanol separation performance of the single-layer TpHZ membranes with different reactive Tp concentration.

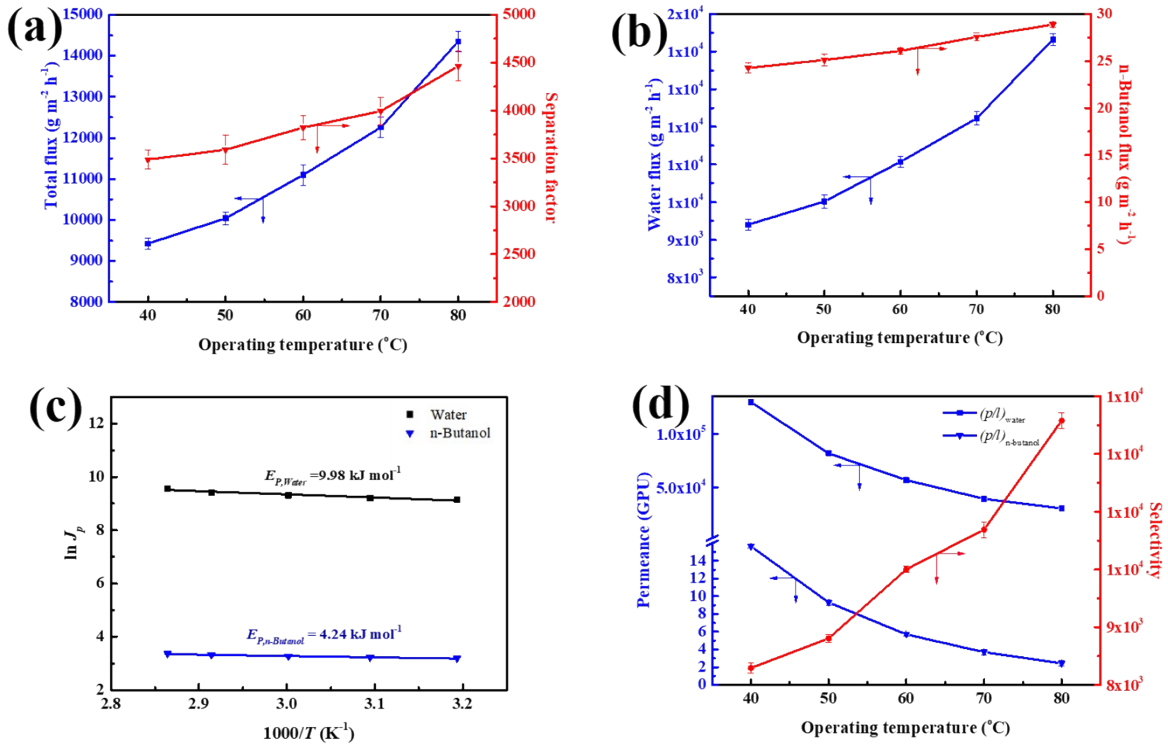


**Fig. S19.** Effect of operating temperature on: (a) total flux and separation factor, (b) water and n-butanol flux, (c) Arrhenius plots of water and n-butanol, and (d) permeance and selectivity of the TpHZ@CTpDHBD membrane for separating 90 wt% n-butanol aqueous solution.

### Note:

To eliminate the influence of pressure, the permeance ( $(P/l)$ , GPU) of the individual component were calculated by equation (S1) and selectivity ( $\beta$ ) is measured by equation (S2).<sup>2</sup>

$$(P/l)_i = \frac{J_i}{p_{i0} - p_{il}} = \frac{J_i}{\gamma_{i0} x_{i0} p_{i0}^{sat} - p_{il}} \quad (\text{S1})$$

$$\beta = \frac{(P/l)_W}{(P/l)_A} \quad (\text{S2})$$

where  $l$  refers to the membrane thickness (m). For individual component  $i$ ,  $J_i$  is the permeation flux ( $\text{kg m}^{-2} \text{ h}^{-1}$ ),  $p_{i0}$  and  $p_{il}$  are the partial pressure (Pa) in the upstream side and the downstream side, respectively.  $\gamma_{i0}$  refers to the activity coefficient which is calculated by the Wilson equation.  $x_{i0}$  is the mole fraction in the feed and  $p_{sat i0}$  is the saturated vapor pressure obtained through the Antoine equation. Subscript  $W$  and  $A$  stand for water and alcohol, respectively.

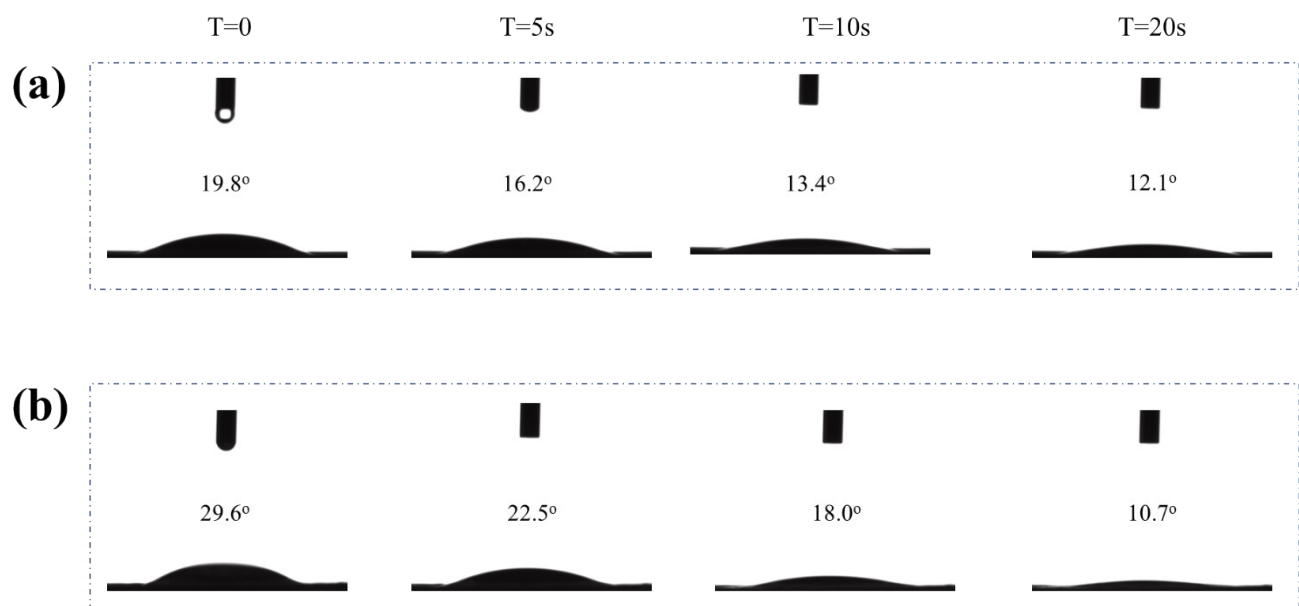


**Fig. S20.** Water contact angles of (a) TpHZ@CTpDHBD membrane and (b) CTpDHBD membrane.

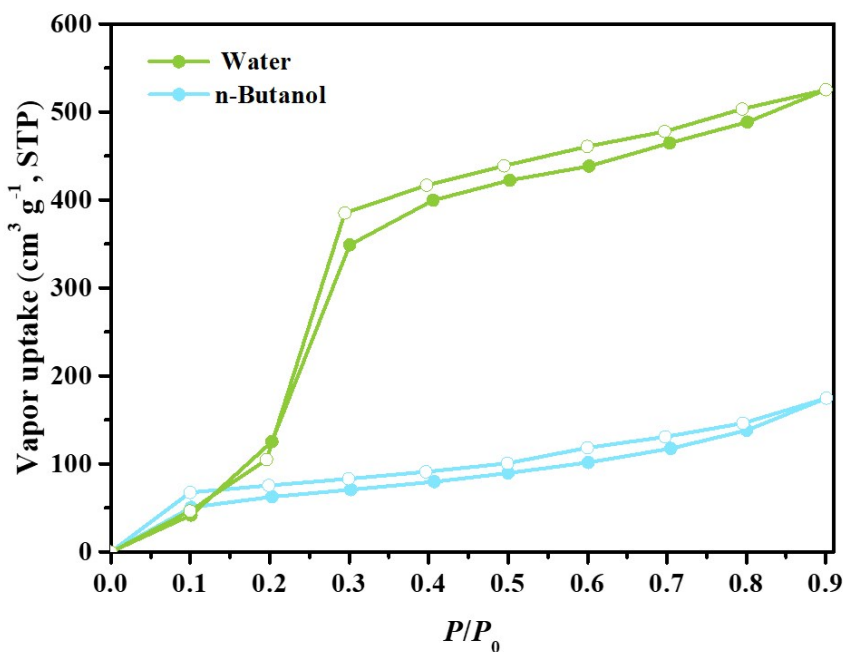


**Fig. S21.** Water and n-butanol vapor adsorption-desorption isotherms (STP) of TpHZ. The filled symbols correspond to adsorption and the un-filled symbols correspond to desorption.

**Note:** The water/alcohol vapor adsorption isotherms of the COFs were collected by a Beishide 3H-2000PW steam adsorption instrument at 298 K. First, the samples were degassed under vacuum at 150 °C for 24 h and then adsorbed water/alcohol vapor at different relative pressure. The weight of the samples was measured in real time until reaching the adsorption equilibrium at each relative pressure. Then the water/alcohol vapor uptake data were collected to obtain the water/alcohol vapor uptake adsorption-desorption isotherms.

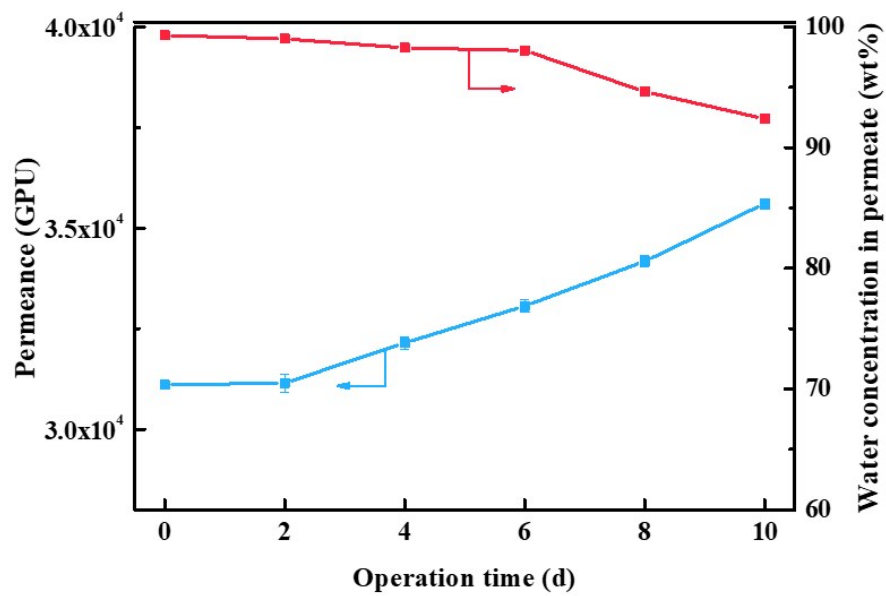


**Fig. S22.** Long-term operation stability of the heterostructured COF membrane fabricated by single vacuum-assisted self-assembly.

## Supplementary Tables

**Table S1.** Chemical element analysis of CTpDHBD.

	C	H	N
Element content (wt%)	62.74	3.85	6.58

**Table S2.** PALS results of the heterostructured COF membrane from LT-9 analysis.

$\tau_3(\text{ns})$	$I_3(\%)$	$\tau_4(\text{ns})$	$I_4(\%)$	$d_3(\text{nm})$	$d_4(\text{nm})$	R-squared
$1.203 \pm 0.019$	$4.1 \pm 0.1$	$3.527 \pm 0.013$	$27.2 \pm 0.3$	$0.392 \pm 0.001$	$0.795 \pm 0.001$	0.9754

**Note:** The third-annihilate lifetime ( $\tau_3$ ) and fourth-annihilate lifetime ( $\tau_4$ ) are derived from the interfacial sub-nanopores and the intrinsic pore of TpHZ. The calculated  $d_3$  and  $d_4$  are in accord with the N<sub>2</sub> adsorption results. The intrinsic pore size of CTpDHBD exceeds the detection limit of PALS with a four-annihilate lifetime spectrum.

**Table S3.** Comparison of the n-butanol dehydration performance of representative membranes reported in literatures and in this study.

Membrane type	Temperature (°C)	Water concentration in feed (wt%)	Permeation flux (kg m <sup>-2</sup> h <sup>-1</sup> )	Separation factor	Reference
Polymeric membrane	60	10	2.24	1116	3
Polymeric membrane	50	5	0.77	481	4
Polymeric membrane	60	15	0.39	2518	5
Polymeric membrane	80	5	0.70	180	6
Polymeric membrane	60	5	0.25	350	7
Polymeric membrane	70	10	1.12	1000	8
Polymeric membrane	60	15	0.85	1174	9
Polymeric membrane	30	13	2.30	3237	10
Mixed matrix membrane	60	15	0.29	14214	11
Mixed matrix membrane	80	10	2.54	2735	12
Mixed matrix membrane	80	10	3.61	2764	13
Silica membrane	60	6	1.50	1000	14
Silica membrane	70	5	2.30	680	15
Silica membrane	60	5	1.21	2811	16
Zeolite membrane	75	5	2.00	1500	17
Zeolite membrane	75	5	3.43	1300	18
GO membrane	70	10	4.34	1791	19
GO membrane	70	10	1.63	5120	20
GO membrane	70	10	10.12	1523	21
GO membrane	50	10	0.70	15000	22
GO membrane	80	10	9.11	2941	23
GO membrane	70	20	3.51	4454	24
MOF membrane	70	5	5.38	4280	25
MOF membrane	60	15	0.08	3417	26
COF membrane	80	10	8.53	3876	1
COF membrane	80	10	10.573	5534	27
COF membrane	80	10	14.35	4464	This work

## Supplementary References

1. H. Yang, L. X. Yang, H. J. Wang, Z. Xu, Y. M. Zhao, Y. Luo, N. Nasir, Y. M. Song, H. Wu, F. S. Pan and Z. Y. Jiang, *Nat. Commun.*, 2019, **10**, 2101.
2. H. Yang, H. Wu, Z. Xu, B. Mu, Z. Lin, X. Cheng, G. Liu, F. Pan, X. Cao and Z. Jiang, *J. Membr. Sci.*, 2018, **561**, 79-88.
3. T. Liu, Q. F. An, Q. Zhao, K. R. Lee, B. K. Zhu, J. W. Qian and C. J. Gao, *J. Membr. Sci.*, 2013, **429**, 181-189.
4. G. J. Zhang, X. Song, S. L. Ji, N. X. Wang and Z. Z. Liu, *J. Membr. Sci.*, 2008, **325**, 109-116.
5. N. Widjojo and T. S. Chung, *Chem. Eng. J.*, 2009, **155**, 736-743.
6. W. F. Guo, T. S. Chung and T. Matsuura, *J. Membr. Sci.*, 2004, **245**, 199-210.
7. W. E. Schehlmann M. S., *J. Membr. Sci.*, 1995, **107**, 277-282.
8. Y. X. Zhu, S. S. Xia, G. P. Liu and W. Q. Jin, *J. Membr. Sci.*, 2010, **349**, 341-348.
9. Y. Wang, S. H. Goh, T. S. Chung and P. Na, *J. Membr. Sci.*, 2009, **326**, 222-233.
10. S. Kalyani, B. Smitha, S. Sridhar and A. Krishnaiah, *Carbohydr. Polym.*, 2006, **64**, 425-432.
11. Y. M. Xu and T. S. Chung, *J. Membr. Sci.*, 2017, **531**, 16-26.
12. H. Yang, H. Wu, Z. Xu, B. W. Mu, Z. X. Lin, X. X. Cheng, G. H. Liu, F. S. Pan, X. Z. Cao and Z. Y. Jiang, *J. Membr. Sci.*, 2018, **561**, 79-88.
13. G. H. Liu, Z. Y. Jiang, H. Yang, C. D. Li, H. J. Wang, M. D. Wang, Y. M. Song, H. Wu and F. S. Pan, *J. Membr. Sci.*, 2019, **572**, 557-566.
14. B. Ben, A. Verhoef, H. M. van Veen, C. Vandecasteele, J. Degreve and B. Van der Bruggen, *Comput. Chem. Eng.*, 2010, **34**, 1775-1788.
15. A. W. Verkerk, P. van Male, M. A. G. Vorstman and J. T. F. Keurentjes, *Sep. Purif. Technol.*, 2001, **22-3**, 689-695.
16. B. X. Huang, Q. Liu, J. Caro and A. S. Huang, *J. Membr. Sci.*, 2014, **455**, 200-206.
17. F. Zhang, L. N. Xu, N. Hu, N. Bu, R. F. Zhou and X. S. Chen, *Sep. Purif. Technol.*, 2014, **129**, 9-17.
18. N. Hu, Y. H. Zheng, Z. Yang, R. F. Zhou and X. S. Chen, *RSC Adv.*, 2015, **5**, 87556-87563.
19. C. H. Tsou, Q. F. An, S. C. Lo, M. De Guzman, W. S. Hung, C. C. Hu, K. R. Lee and J. Y. Lai, *J. Membr. Sci.*, 2015, **477**, 93-100.
20. G. H. Li, L. Shi, G. F. Zeng, Y. F. Zhang and Y. H. Sun, *RSC Adv.*, 2014, **4**, 52012-52015.
21. K. Huang, G. Liu, J. Shen, Z. Chu, H. Zhou, X. Gu, W. Jin and N. Xu, *Adv. Funct. Mater.*, 2015, **25**, 5809-5815.
22. J. J. Yang, D. A. Gong, G. H. Li, G. F. Zeng, Q. Y. Wang, Y. L. Zhang, G. J. Liu, P. Wu, E. Vovk, Z. Peng, X. H. Zhou, Y. Yang, Z. Liu and Y. H. Sun, *Adv. Mater.*, 2018, **30**, 1705775.
23. Y. M. Song, R. Li, F. S. Pan, Z. He, H. Yang, Y. Li, L. X. Yang, M. D. Wang, H. J. Wang and Z. Y. Jiang, *J. Mater. Chem. A*, 2019, **7**, 18642-18652.
24. Y. Y. Mao, M. C. Zhang, L. Cheng, J. W. Yuan, G. P. Liu, L. B. Huang, M. Barboiu and W. Q. Jin, *J. Membr. Sci.*, 2020, **595**, 10.
25. X. L. Liu, C. H. Wang, B. Wang and K. Li, *Adv. Funct. Mater.*, 2017, **27**, 1604311.
26. G. M. Shi, T. X. Yang and T. S. Chung, *J. Membr. Sci.*, 2012, **415**, 577-586.
27. H. J. Wang, L. Chen, H. Yang, M. D. Wang, L. X. Yang, H. Y. Du, C. L. Cao, Y. X. Ren, Y. Z. Wu, F. S. Pan and Z. Y. Jiang, *J. Mater. Chem. A*, 2019, **7**, 20317-20324.